

## Undergraduate experiments on statistical optics

This content has been downloaded from IOPscience. Please scroll down to see the full text.

2016 Eur. J. Phys. 37 055302

(<http://iopscience.iop.org/0143-0807/37/5/055302>)

View [the table of contents for this issue](#), or go to the [journal homepage](#) for more

Download details:

IP Address: 130.75.102.234

This content was downloaded on 03/03/2017 at 14:40

Please note that [terms and conditions apply](#).

You may also be interested in:

### ON THE USE OF SHOT NOISE FOR PHOTON COUNTING

Jonas Zmuidzinas

Simulation study of the impact of AGIPD design choices on X-ray Photon Correlation Spectroscopy utilizing the intensity autocorrelation technique

J Becker, C Gutt and H Graafsma

Experimental determination of the correlation properties of plasma turbulence using 2D BES systems

M F J Fox, A R Field, F van Wyk et al.

Fluctuations of Photon Beams and their Correlations

L Mandel

From quantum to thermal topological-sector fluctuations of strongly interacting Bosons in a ring lattice

Tommaso Roscilde, Michael F Faulkner, Steven T Bramwell et al.

Dynamical modeling of pulsed two-photon interference

Kevin A Fischer, Kai Müller, Konstantinos G Lagoudakis et al.

Collective dynamics of multimode bosonic systems induced by weak quantum measurement

Gabriel Mazzucchi, Wojciech Kozłowski, Santiago F Caballero-Benitez et al.

Covariance mapping techniques

Leszek J Frasinski

Correlation-induced spectral changes

Emil Wolf and Daniel F V James

# Undergraduate experiments on statistical optics

Ruediger Scholz<sup>1</sup>, Gunnar Friege<sup>2</sup> and Kim-Alessandro Weber<sup>2</sup>

<sup>1</sup>Institut für Quantenoptik, Leibniz Universität Hannover, D-30167 Hannover, Germany

<sup>2</sup>Institut für Didaktik der Mathematik und Physik, Leibniz Universität Hannover, D-30167 Hannover, Germany

E-mail: [r.scholz@iqo.uni-hannover.de](mailto:r.scholz@iqo.uni-hannover.de)

Received 7 April 2016, revised 16 May 2016

Accepted for publication 26 May 2016

Published 24 June 2016



CrossMark

## Abstract

Since the pioneering experiments of Forrester *et al* (1955 *Phys. Rev.* **99** 1691) and Hanbury Brown and Twiss (1956 *Nature* **177** 27; *Nature* **178** 1046), along with the introduction of the laser in the 1960s, the systematic analysis of random fluctuations of optical fields has developed to become an indispensable part of physical optics for gaining insight into features of the fields. In 1985 Joseph W Goodman prefaced his textbook on statistical optics with a strong commitment to the ‘tools of probability and statistics’ (Goodman 2000 *Statistical Optics* (New York: John Wiley & Sons Inc.)) in the education of *advanced* optics. Since then a wide range of novel undergraduate optical counting experiments and corresponding pedagogical approaches have been introduced to underpin the rapid growth of the interest in coherence and photon statistics. We propose low cost experimental steps that are a fair way off ‘real’ quantum optics, but that give deep insight into random optical fluctuation phenomena: (1) the introduction of statistical methods into undergraduate university optical lab work, and (2) the connection between the photoelectrical signal and the characteristics of the light source. We describe three experiments and theoretical approaches which may be used to pave the way for a well balanced growth of knowledge, providing students with an opportunity to enhance their abilities to adapt the ‘tools of probability and statistics’.

Keywords: quantum optics, optics, statistical optics, photoelectron statistics, advanced optics, undergraduate lab, fluctuations

## 1. Motivation

Light is an electromagnetic phenomenon and Maxwell's equations lead to the powerful classical electro-dynamical optical theory (CED). It governs the total range of wave optics: diffraction, interference and optical coherence, semi-classical atomic spectroscopy and even nonlinear phenomena. As shown in a standard and famous textbook, the electromagnetic theory [15] of the short wave length limit, together with the Schwarzschild eikonal theory, provides access to geometrical optics. Consequently most students at the sophomore level experienced optical science in physics merely restricted to a deterministic framework. Noise is regarded as a fault and classical optical quantities are assumed to be precisely measurable—at least in principle.

Two central arguments are well known, revealing the fallacy.

1. In almost all optical experiments light is emerging from a random sample of excited atoms, thus *light is a result of a statistical process* and controlled by random variables. Teaching optics solely on the basic of CED ignores this fact and undervalues the information hidden in noise and fluctuation.
2. In an early statement Einstein demonstrated the statistical nature of radiation [5]. He analysed the statistical noise of radiation fields in thermal equilibrium. As a measure for the noise he determined the *variance* of the energy (see appendix A for details of the calculation)

$$\langle \Delta W^2 \rangle = \langle (W - \langle W \rangle)^2 \rangle \Rightarrow \langle \Delta W^2 \rangle = k_B T^2 \cdot \left( \frac{\partial \langle W \rangle}{\partial T} \right)_V. \quad (1)$$

Now inserting Planck's formula for the mean energy  $\langle W \rangle$  of the radiation field at absolute temperature  $T$  with a frequency  $f = \omega/2\pi$ , we identify the classical behaviour and quantum mechanical characteristics of the blackbody radiation

$$\begin{aligned} \langle W \rangle &= V \cdot \frac{\hbar \omega^3}{\pi^2 c^3} \frac{1}{\exp(\hbar \omega / k_B T) - 1} \Rightarrow \langle \Delta W^2 \rangle = \left( \hbar \omega + \frac{\pi^2 c^3}{V \omega^2} \langle W \rangle \right) \langle W \rangle \Rightarrow \\ \frac{\langle \Delta W^2 \rangle}{\langle W \rangle^2} &= \left( \frac{\hbar \omega}{\langle W \rangle} + \frac{\pi^2 c^3}{V \omega^2} \right). \end{aligned} \quad (2)$$

The two terms within the round brackets are completely different in principle: the first one,  $\hbar \omega / \langle W \rangle$ , gives the quantum contribution to the fluctuations due to the distinct character of the energy exchange between the radiation field and the matter; the second one,  $\pi^2 c^3 / (V \omega^2)$ , originates from thermal fluctuations of the classical electromagnetic field. The first term vanishes for small  $\omega$  (thus the quantum character of radio waves might be neglected). The second term vanishes for high frequencies. Physical optics in this region is governed by photonics and photoelectron statistics.

Equation (2) elucidates the important fact that in the limit  $\hbar \omega \gg k_B T$  quantum effects will enter the stage: ignoring the second term in the very high frequency regime and inserting the mean value of the radiation energy  $\langle W \rangle = N \cdot \hbar \omega$  we find  $\langle \Delta W^2 \rangle / \langle W \rangle^2 = 1/N$  instead of equation (2). This supports the fact that in the limit  $\hbar \omega \gg k_B T$  cavity radiation behaves like a sample of independent particles.

Statistical methods for determining the detector response on intercepted radiation and the introduction into methods of probability spectroscopy turn out to be indispensable for gaining insight into the fundamentals of light phenomena.

## 2. The statistical correlation between optical fields and photoelectrons

Following a widely used approach [6] we introduce the following set of helpful parameters (numerical values are from NIST: <http://physics.nist.gov/cuu/Constants/index.html>).

$\langle \Delta X^2 \rangle$	Variance of $X$	$\langle (X - \langle X \rangle)^2 \rangle$
$I_{ca}(t)$	the <i>cycle averaged intensity</i> of the radiation, averaged over one period $2 \cdot \pi / \omega$	$I_{ca} = \frac{\omega}{2\pi} \int_t^{t+2\pi/\omega} dt' I(t')$
$\xi$	efficiency of the detector; connecting the number $m$ of photoelectrons and the intensity $I_{ca}(t)$ of the incoming light	$m(t, \tau_D) = \xi \tau_D I_{ca}(t, \tau_D)$
$\tau_D$	detector sampling period, defining the sample period averaged intensity $I_{ca}(t, \tau_D)$	$I_{ca}(t, \tau_D) = \frac{1}{\tau_D} \int_t^{t+\tau_D} dt' I_{ca}(t')$

The *coherence volume* given by  $V_C = A_C \cdot c \cdot \tau_C$  ( $c$  is the speed of light;  $\tau_C$  is the coherence time,  $A_C$  is the transverse coherence cross section) estimates the spatial expansion of so called *coherence cells* and are sometimes referred to as *independent radiation modes* or *optical degrees of freedom* [6]. The *cycle averaged intensity*  $I_{ca}(t)$  of the radiation is introduced to take into account the fact that a photodetector cannot respond at optical frequencies.  $I_{ca}(t)$  is correlated with the number of  $N$  of photons by

$$I_{ca}(t) = \frac{N \cdot \hbar \omega}{A_C c \tau_D} c = \beta \cdot N. \quad (3)$$

The efficiency  $\xi$  characterises the detection system. Throughout the paper we assume that the probability of producing one single photo count during time  $t$  and  $t + dt$  is given by [8]

$$p(t)dt = \xi I_{ca}(t)dt. \quad (4)$$

Thus we obtain a linear correlation between the sample time averaged intensity  $I_{ca}(t, \tau_D) = \frac{1}{\tau_D} \int_t^{t+\tau_D} dt' I_{ca}(t')$  reaching the detector during the sampling period  $\tau_D$  and the number of measured photo counts  $m$

$$m(t, \tau_D) = \xi \tau_D I_{ca}(t, \tau_D). \quad (5)$$

The basic idea is to find a correlation between the incoming radiation intensity and the distribution of photo counts  $P(m, t, \tau_D)$  measured by the detection set-up [7].

‘Consider a beam of light falling on some photoelectric detector, where photoelectrons are ejected in a certain time interval  $T$ . Only the photoelectrons and not the photons are, of course, observable and our discussion must therefore be confined to the statistical behaviour of the photoelectrons.’ (Mandel 1958 [7])

This perspective gives the guideline for our educational approach: there is a considerable probability that the characteristics of the detector output give insight into the characteristics of the incident radiation. And, low-cost experiments for the undergraduate level can easily be set up to show these characteristics.

In the most common case a constant intensity leads to a Poisson distribution of photo counts (see equation (B5))

$$P(m, t, \tau_D) = \frac{\langle m(t, \tau_D) \rangle^m}{m!} \exp(-\langle m(t, \tau_D) \rangle). \quad (6)$$

$\langle m(t, \tau_D) \rangle$  gives the mean number of counts at time  $t$  averaged over the sampling time  $\tau_D$ . Due to fluctuations of the light incident on the PM, the  $t$ -dependence of  $\langle m(t, \tau_D) \rangle$  is substantially

difficult to determine theoretically. The complete solution is given in [4, 6]. Let us review the basic steps of the argument.

### 2.1. Intensity fluctuations

Due to temporal fluctuations of the intensity  $I_{ca}(t)$  the PM-signal  $m$  could be thought as the result of a temporal mean of signals intercepted by the detector at different points in time  $t$ . Instead of equation (6) we get with  $m(t, \tau_D)$  given by  $m(t, \tau_D) = \xi \cdot I_{ca}(t, \tau_D) \cdot \tau_D$

$$\begin{aligned} P(m, \tau_D) &= \langle P(m, t, \tau_D) \rangle_t = \left\langle \frac{\langle m(t, \tau_D) \rangle^m}{m!} \exp(-\langle m(t, \tau_D) \rangle) \right\rangle_t \\ &= \left\langle \frac{\langle \xi \tau_D I_{ca}(t, \tau_D) \rangle^m}{m!} \exp(-\langle \xi \tau_D I_{ca}(t, \tau_D) \rangle) \right\rangle_t. \end{aligned} \quad (7)$$

### 2.2. Appropriate averaging

Though it is a formidable task to carry out the averaging process in general, sometimes we find arguments to facilitate the calculation. If the fluctuations of the incoming light are stochastically independent we may replace the  $t$ -average by an intensity-average. Let  $P(I_{ca}) dI_{ca}$  be the probability to find the intensity  $I_{ca}$  of the optical field within the range  $I_{ca}$  to  $I_{ca} + dI_{ca}$ , then we find the distribution of photo counts to be given by

$$P(m, \tau_D) = \int_0^\infty dI_{ca} P(I_{ca}) \frac{(\xi \tau_D I_{ca})^m}{m!} \exp(-\xi \tau_D I_{ca}). \quad (8)$$

If we know the probability distribution of the incoming light we can determine the probability distribution of the detector counts. Equation (8) sometimes is referred to as *Poisson transform* [6].

### 2.3. The probability $P(I_{ca}) dI_{ca}$

Four important cases may be identified, solvable with less effort [4, 6].

Case 1. For a constant intensity of an ideal laser we have a delta function like probability function (PF)

$$P(I_{ca}) dI_{ca} = \delta(I_{ca} - I_{laser}) dI_{ca}. \quad (9)$$

Case 2. A chaotic radiation field with a coherence time  $\tau_C$  much greater than the sampling period  $\tau_D$  yields

$$P(I_{ca}) dI_{ca} = \frac{1}{\langle I_{ca} \rangle} \exp\left(-\frac{I_{ca}}{\langle I_{ca} \rangle}\right) dI_{ca}. \quad (10)$$

Case 3. For a very long sampling period all fluctuations will wash out and we again may argue with constant intensity to get the PF

$$P(I_{ca}) dI_{ca} = \delta(I_{ca} - \langle I_{ca} \rangle) dI_{ca}. \quad (11)$$

Case 4. The coherent-cell-concept is helpful in the medium  $\tau_D$ -range. This concept describes the integrated intensity  $I_{ca}$  as the sum of  $q$  independent exponentially distributed

modes (see case 2) lumped together by the detector during the sampling period [6] ( $\Gamma(q)$  represents the Euler gamma function)

$$P(I_{ca}(t, \tau_D))dI_{ca} = \frac{q^q}{\Gamma(q)} \frac{I_{ca}(t, \tau_D)^{q-1}}{\langle I_{ca}(t, \tau_D) \rangle^q} \exp\left(-\frac{qI_{ca}(t, \tau_D)}{\langle I_{ca}(t, \tau_D) \rangle}\right) dI_{ca}, \quad (12)$$

$q_S$  depends on the spatial coherence of the radiation and thus strongly on characteristics of the radiation (see [6] for details of the calculation).

#### 2.4. The statistics of photo counts

Inserting equations (9)–(12) into equation (8) gives the final result

$$\begin{aligned} & P(m, \tau_D) \\ &= \int_0^\infty dI_{ca} P(I_{ca}) \frac{(\xi \tau_D I_{ca})^m}{m!} \exp(-\xi \tau_D I_{ca}) \\ &= \begin{cases} \{1\}: \frac{\langle m \rangle^m}{m!} \exp(-\langle m \rangle); & \tau_C \gg \tau_D; \langle m \rangle = \xi \tau_D I_{laser} \\ \{2\}: \frac{\langle m \rangle^m}{(1 + \langle m \rangle)^m}; & \tau_C \gg \tau_D; m(t, \tau_D) = \xi \tau_D \frac{1}{\tau_D} \int_t^{t+\tau_D} dt' I_{ca}(t') \\ \{3\}: \frac{\langle m \rangle^m}{m!} \exp(-\langle m \rangle); & \tau_C \ll \tau_D; \langle m \rangle = \xi \tau_D \langle I_{ca} \rangle \\ \{4\}: \frac{\Gamma(m+q)}{m! \Gamma(q)} \frac{1}{\left(1 + \frac{q}{\langle m \rangle}\right)^m} \\ & \cdot \frac{1}{\left(1 + \frac{\langle m \rangle}{q}\right)^q}; & \tau_C > \tau_D; m(t, \tau_D) = \xi \tau_D \frac{1}{\tau_D} \int_t^{t+\tau_D} dt' I_{ca}(t') \end{cases} \quad (13) \end{aligned}$$

To illustrate the mathematics behind it, some of the basic calculations are shown in the appendix.

We will study three of these four cases with three different low cost experiments designed for our undergraduate approach to statistical optics. Case 1 has been reported elsewhere [13]. There we used a Mach–Zehnder-set-up to measure the Poisson distributed light from the laser.

**2.4.1. Experiment 1: basic laws of counting with x-rays.** This first experiment focuses on case 3, counting photoelectrons in x-ray-experiments. The basic experimental set-up itself is well known in undergraduate physics education. The new idea is its role within the framework of statistical optics: we use this experiment together with the analysis based on Mandel's formula (equation (8)) to introduce the very first steps of optical counting. While the most common perspective takes the clicks from the binary counter simply as the direct measure of the incoming x-ray-radiation, our (theoretical) approach aims at taking a first glance at the correlation between the photoelectrical signal and the radiation source in a much more generalizable sense.

**2.4.2. Experiment 2: influence of coherence.** The second experiment demonstrates a way to produce light characterised by case 2, showing that coherence characteristics might be

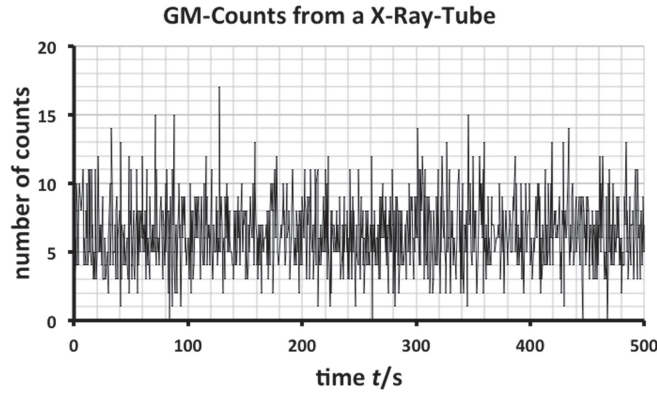


**Figure 1.** Time series of the number  $m$  of pulses from a GM-device during  $\tau_D = 500$  ms (10 000 records from a Phywe x-ray Cu-anode, 14 kV,  $i = 0.1$  mA, LiF glancing angle  $\theta = 23^\circ$ ; GM-tube is running in the Geiger modus), the first 500 records are shown. This time series clearly shows the typical asymmetry of the Poissonian and a mean value greater than zero. It should be compared with figure 4.

accessible by a probabilistic view on wave characteristics. The experiment recreates a former set-up introduced in the early days of speckle spectroscopy [5]. We used the set-up to demonstrate the effect of mixing coherent and pseudo thermal light.

**2.4.3. Experiment 3: pseudo-thermal intensity fluctuations with LED.** A modern LED provides a low cost light source with many remarkable features: a very small relaxation time in the semiconductor, a considerable coherence length of a few  $\mu\text{m}$  and extraordinary simple operation electronics makes it an appropriate tool in statistical optical analysis. We use this light source to produce case 4-light with different  $q$ -values.

### 3. The experiments

#### 3.1. Experiment 1: basic laws of counting with x-rays

Experiments with this set up are well suited to give insight into basic counting mechanisms. Although safety and experimental requirements are higher for x-ray experiments than for experiments with visible light, the advantage of the x-ray experiment is the availability of the materials in many regular labs for students and students who are acquainted with traditional x-ray-set-ups. Geiger–Muller (GM)-tube-devices work as binary detectors counting the number of clicks during some detection period  $\tau_D$ . The resulting time series turns out to be noisy (figure 1).

A pulse counting histogram analysis of the GM-output is used to investigate the fluctuations. We checked the experimental distribution of the frequency of occurrence (figure 2) and found it coincided well with a Poisson probability function (PF).

To explain the results referring to statistical optics we may argue as follows. For a GM-counter running in the GM-mode we assume a detector efficiency  $\xi \approx 1$ ; each voltage pulse from the GM-counter (each ‘click’) counts exactly one energy package reaching it. Due to the long sampling period of the detector,  $\tau_D = 500$  ms, the fluctuations of the x-ray-tube cancel out and the intensity does not depend on  $t$  (the coherence length of the 35 keV-CuK $_{\alpha 1}$ -line is about 400 nm corresponding to  $\tau_C \approx 1.3 \cdot 10^{-15}$  s)

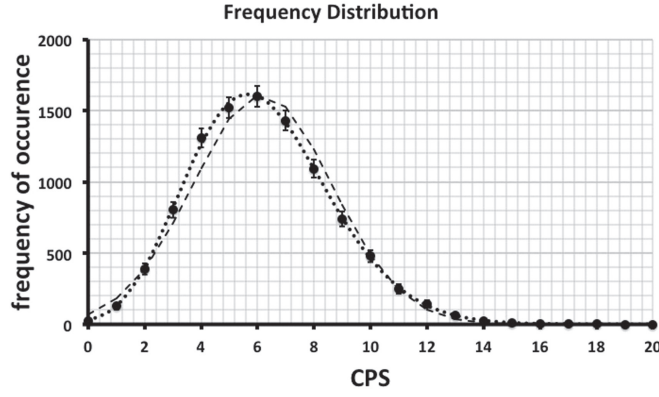


**Figure 2.** Pulse-counting-histogram-analysis of the times series gives the probability function  $P(m)$  of the number of counts measured during 500 ms with a mean value  $\langle m \rangle = 6.17$  and with a variance  $\sigma^2(m) = 6.15$ . Error bars give the standard error of the frequency of occurrence. Big dots show the experimental values from figure 1, the dotted line shows the theoretical Poisson distribution  $P_{\text{poi}}(m; \langle m \rangle)$ ; the mean deviation between the theoretical values and the measurement is given by the rms-value  $\Delta p = 15$ . The occurrence is not Gaussian distributed, as can be seen from the dashed line.

$$I_{\text{ca}}(t, \tau_{\text{D}}) = \frac{1}{\tau_{\text{D}}} \int_t^{t+\tau_{\text{D}}} dt' I_{\text{ca}}(t') = I_{\text{ca}}(\tau_{\text{D}}) = \text{const.} \Rightarrow \quad (14)$$

$$\langle m \rangle = \xi \tau_{\text{D}} \langle I_{\text{ca}}(t, \tau_{\text{D}}) \rangle = \xi \tau_{\text{D}} I_{\text{ca}}(\tau_{\text{D}}).$$

The probability distribution is easily calculated

$$P(m, \tau_{\text{D}}) = \langle P(m, t, \tau_{\text{D}}) \rangle_t = \left\langle \frac{(\xi \tau_{\text{D}} I_{\text{ca}}(t, \tau_{\text{D}}))^m}{m!} \exp(-\xi \tau_{\text{D}} I_{\text{ca}}(t, \tau_{\text{D}})) \right\rangle_t$$

$$= \frac{(\xi \tau_{\text{D}} I_{\text{ca}}(\tau_{\text{D}}))^m}{m!} \exp(-\xi \tau_{\text{D}} I_{\text{ca}}(\tau_{\text{D}})) = \frac{\langle m \rangle^m}{m!} \exp(-\langle m \rangle). \quad (15)$$

Figures 1 and 2 show the experimental results. The photoelectrons are obviously Poisson distributed (see figure 2); the fit (dotted line) uses  $\langle m \rangle = 6.17$ . Due to a long integration time  $\tau_{\text{D}}$  most details of the radiation are washed out.

*Hint:* non ideal features of the counter affect the result. The x-ray tube should be run in the low intensity regime, because for x-ray intensities above the boundaries given by the dead-time-limit of the GM-counter the distribution  $P(m, \langle m \rangle)$  measured in this experiment will differ significantly from the Poissonian.

### 3.2. Experiment 2: influence of coherence

To gain insight into more detailed features of the radiation we might use a sampling time below the coherence time  $\tau_{\text{C}}$ , i.e. case 2. For this purpose we analysed diffuse scattered coherent light from a laser.

In optics and quantum optics the definition of coherence relies on the visibility of interference [8].

- The coherence time  $\tau_{\text{C}}$  can be measured by the maximum delay in a Michelson interferometer before the pattern vanishes.

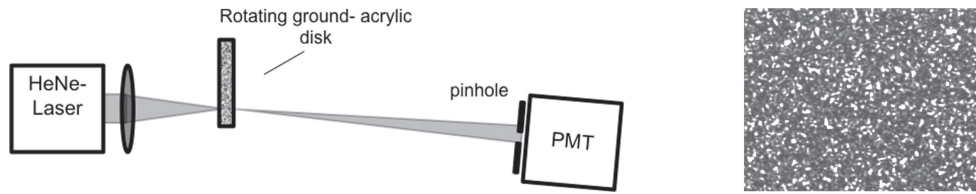


**Figure 3.** Sketch of set up of the speckle experiment.

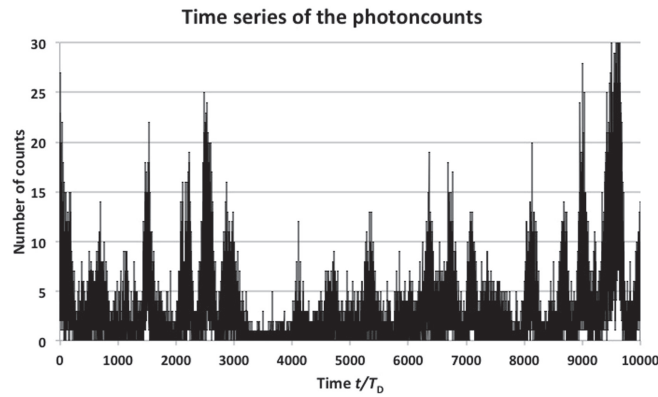


**Figure 4.** Typical time series of the photon counts;  $\tau_D = 1 \cdot 10^{-4}$  s.

- From the analysis of the power density of the radiation one finds  $\tau_C \approx 1/\Delta f$  with a radiation bandwidth  $\Delta f$ .
- Spatial coherence is determined from Young's double slit experiment: the transverse coherence area  $A_C$  is given by the maximum separation of the slits to wash out the interference pattern.
- In modern optics these phenomena are referred to as first order coherence (coherence of the *fields*). The volume of the so called coherence cell is given by  $V_C = A_C \cdot c \cdot \tau_C$ .

In 1964 Martienssen and Spiller demonstrated that laser radiation scattered by a rotating ground-glass behaves like a thermal light with extraordinary long coherence time  $\tau_C$  depending on the rotation velocity, so called *pseudo-thermal* light [9]. Focusing the laser on the ground glass will produce a random speckle pattern (figure 3).

The mean size of the speckles may be determined from a random phasor model very similar to the one exemplified in appendix D. By treating speckles as a random-walk phenomenon the distribution of scale sizes in a speckle pattern can be calculated [14]. Details of these calculations however exceed the undergraduate framework of the description given here. In our experiment we found a mean diameter  $d \approx 2$  mm. Due to the random structure of the diffuser the spatial coherence between two speckles is completely lost. Thus we have a coherence volume given by the mean speckle size:  $V_C = A_C \cdot c \cdot \tau_C \approx d^2 \cdot c \cdot \tau_C$ . Now let us observe the fluctuation from a single speckle-sized region. Regarding each speckle as an independent light source, a moving speckle pattern might be regarded as random fluctuating light. In fact, rotating the diffuser, the intensity of the light reaching the observer (see figure 4) shows temporal fluctuations very similar to thermal light as described in [8].

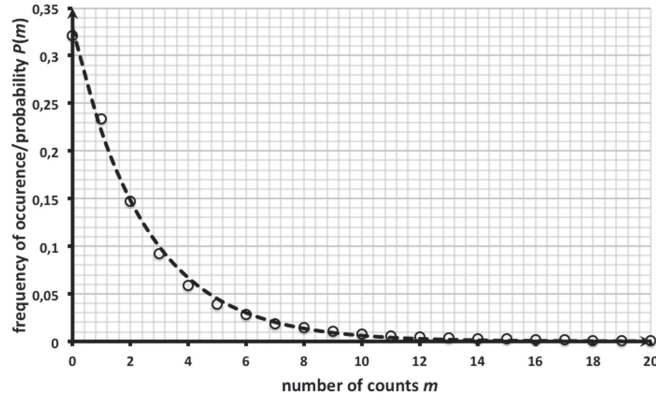


**Figure 5.** Relative frequency of occurrence (open circles); the dashed line shows the negative exponential distribution expected here (see equation (10) and appendix C);  $\langle m \rangle = 2.04$ .

Referring to classical field theory intensity fluctuations  $I_{ca}(t)$  of the light from thermal sources (class-2-light) are explained from randomly distributed phase interruptions in the light waves emitted. It could be shown that the technique of optical counting is appropriate to detect these fluctuations and deduce coherence properties, provided that the sampling time of the detector is short compared to the coherence time. Otherwise temporal averaging will wash out the short-time fluctuations [8, p 83 ff].

For the set-up shown in figure 3 we could realize a time of constant phase  $\tau_C$ , given by the round trip period of the disk ( $\tau_\omega = 2\pi/\omega$ ), the speckle size  $d$  and the speckle position  $R$  from the centre of rotation

$$\tau_C = \frac{d}{2\pi R} \cdot \tau_\omega \approx 4 \cdot 10^{-6} \cdot \tau_\omega. \quad (16)$$

Figure 5 shows the result: a perfect geometrical distribution for the photoelectric counts as expected for thermal chaotic light. Starting with the probability function of the photo-counts  $P(m, \tau_D)$  we can calculate the probability function of the intensity  $P(I_{ca})dI_{ca}$  using  $\langle m \rangle = \xi \cdot \tau_D \cdot \langle I_{ca} \rangle$  (see appendix C; equation (C8) with  $q = 1$ ) to find the exponential equation (10) (case 2).

### 3.3. Experiment 3: pseudo-thermal intensity fluctuations with LED

**3.3.1. Part A: a perfect Poissonian from constant intensity (case 3).** So far we have demonstrated two limiting regions of the detection period  $\tau_D$ :

- if  $\tau_D$  is long compared to the coherence time  $\tau_C$  we find Poisson distributed photo counts (equation (4));
- if  $\tau_D$  is short compared to  $\tau_C$  we find the pseudo-thermal geometrical probability function (equation (6)).

Our next experiment will illuminate the region of arbitrary sampling time between these limits. Due to the characteristics of the electroluminescence, LEDs turn out to be ideal low cost light sources with an intensity that is easy to modulate via the modulation of the electrical current [12]. The maximum modulation frequency of the LED is obviously restricted by the response time  $\tau_R$  at which the recombination of minority carriers, injected into the pn-

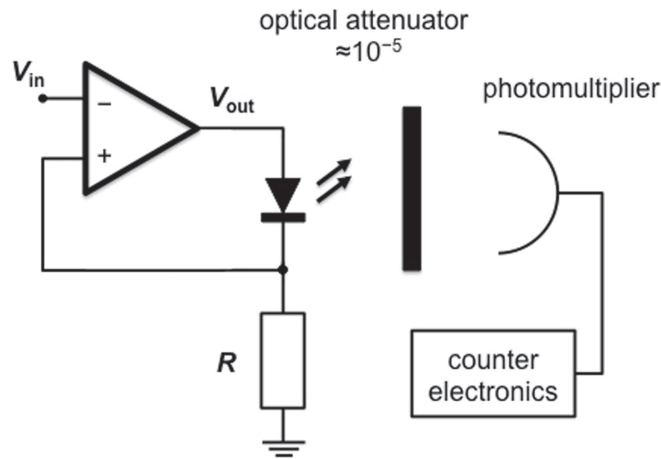


**Figure 6.** LED experiments; overview of the experimental apparatus.

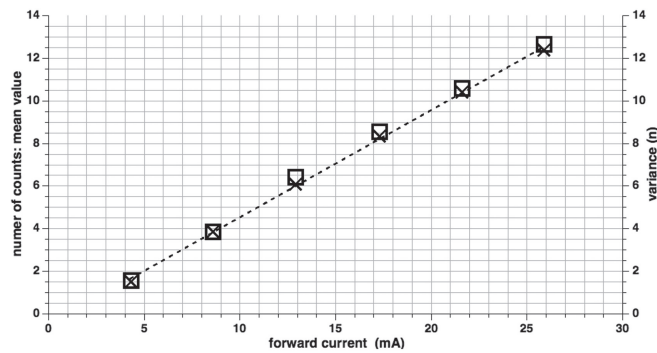


**Figure 7.** LED experiments; number of photo counts as a function of the LED-forward current  $4.3 < I < 25.9$  mA;  $\tau_D = 20 \cdot 10^{-6}$  s. Crosses show the mean value  $\langle m \rangle$  (left ordinate axis) and squares show the variance  $\langle \Delta m^2 \rangle \approx \langle m \rangle$ , as expected (right ordinate axis), the dotted line shows a linear regression of the mean values (slope  $0.503 \text{ mA}^{-1}$ ;  $R^2 = 0.999$ ).

junction, occurs. Typical values of  $1 \text{ ns} < \tau_R < 50 \text{ ns}$  giving a cut-off frequency of some hundreds of MHz.

Our experimental set up is shown in figure 6: the light from a red LED (L-53SR SUPER BRIGHT RED,  $\lambda_{\text{centre}} = 660 \text{ nm}$ ;  $4.3 < I < 25.9 \text{ mA}$ ) could arbitrarily be modulated (bandwidth  $< 0.5 \text{ MHz}$ ). The use of a voltage to constant-current converter assures the appropriate operation of the LED. By using a homebuilt D/A-converter the controlling voltage could be varied with a  $1/255$ -step-range increment. To reduce the light intensity ( $\approx 10^{-5}$ ) we combined an optical polarizer and simple neutral density (ND) filters. Thus we could reduce the theoretical effort confining the analysis to the case of polarized light.

The signal has been measured by a PM-equipment (maximum  $\approx 100$  to  $200$  counts per  $20 \mu\text{s}$ ) and could be analysed via standard counter electronics (discriminator plus digital counter electronics).

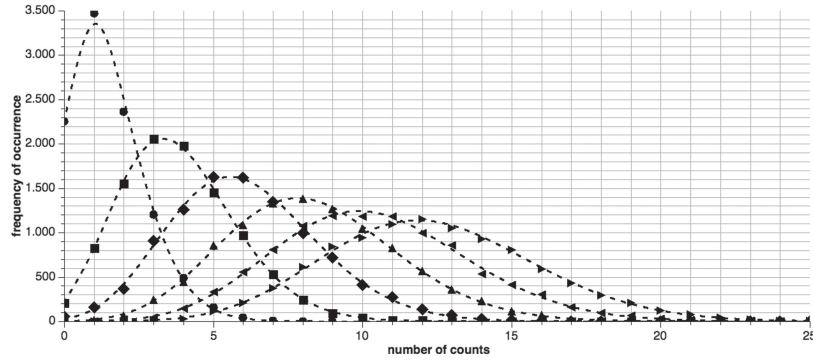


**Figure 8.** The occurrence of photoelectrons: the probability distribution of counts measures for a forward current  $i = 4.3$  mA, 8.6 mA, 12.9 mA, 17.3 mA, 21.6 mA, 25.9 mA; the dotted lines are the theoretical Poissonian calculated from the respective measured mean values. The fit is evident.

For a forward current not exceeding a maximum value, depending on the specific type of LED (in our case we had  $I < 25.9$  mA) the light intensity  $I_{ca}(t)$  of the LED can simply be written as  $I_{ca} = \alpha \cdot i$  with a total conversion efficiency  $\alpha$  not depending on the current.

Results of the experiment part A show this overall linearity of the light modulation set up (figure 7). Here we measured 10 000 records of photoelectrons from the PM-counter as a function of the constant operating LED-current  $i$ . Figure 7 shows as the result the mean value  $\langle m \rangle$  and the variance  $\langle \Delta m^2 \rangle = \langle m^2 \rangle - \langle m \rangle^2$  from these data sets. It shows the remarkable linearity of the mean as a function of the operating current  $i$ . The variance (squares in figure 7) is obviously given by the mean:  $\langle \Delta m^2 \rangle = \langle m^2 \rangle - \langle m \rangle^2 = \langle m \rangle$ , giving reasonable clues that we are dealing with a Poissonian distribution. In fact, for the constant-current case we expect the photoelectrons from the PM to be Poisson distributed (see equation (B5))

$$P(m, t, \tau_D) = \frac{\langle m(t, \tau_D) \rangle^m}{m!} \exp(-\langle m(t, \tau_D) \rangle); \quad \langle m \rangle = \xi \cdot \tau_D \cdot \langle I_{ca} \rangle. \quad (17)$$

We found the Poisson distribution of photo counts over a wide range of intensities  $I_{ca}$ . Figure 8 shows some examples for  $4.3 \text{ mA} < I < 25.9 \text{ mA}$  proving the perfect match between theory and experiment.

### 3.4. Experiment 3: pseudo-thermal intensity fluctuations with LED

**3.4.1. Part B: fluctuations of light from a pseudo-thermal modulated LED (case 4).** Part B of experiment 3 has been designed to analyse random fluctuations of the intensity in a more detailed manner. Using the high modulation capability of the LED-intensity, the LED-experiments give the opportunity to produce pseudo-thermal light with variable statistical characteristics. For this purpose we have developed the experimental analogue of a one dimensional random phasor model for the forward current (see [4] and appendix D for a detailed description).

We start with the circularly complex distributed random variable  $A = AX + iAY$  (figure 9). From elementary statistics we know [4] that the absolute value (the phasor length  $|A|$ ) is Rayleigh distributed

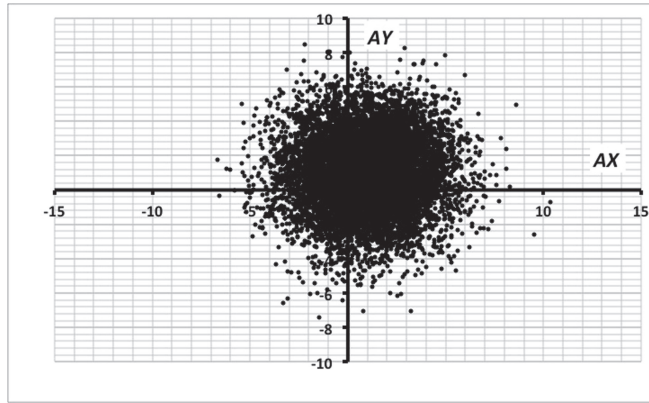


**Figure 9.** The random phasor model. Each dot gives the arrow-head for a complex phasor  $A = AX + iAY$ ; with  $\langle AX \rangle = \langle AY \rangle = 0.5$  and  $\sigma(AX) = \sigma(AY) = 2.1$ .

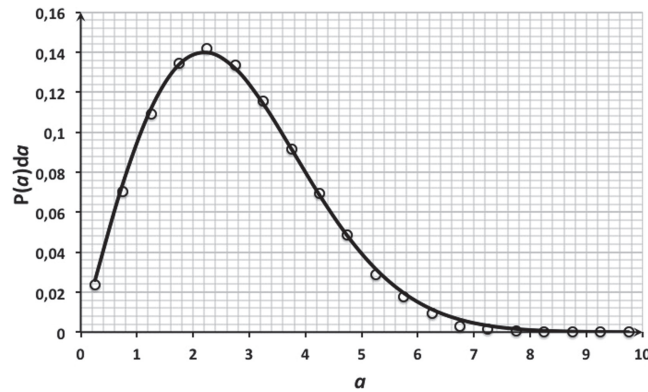
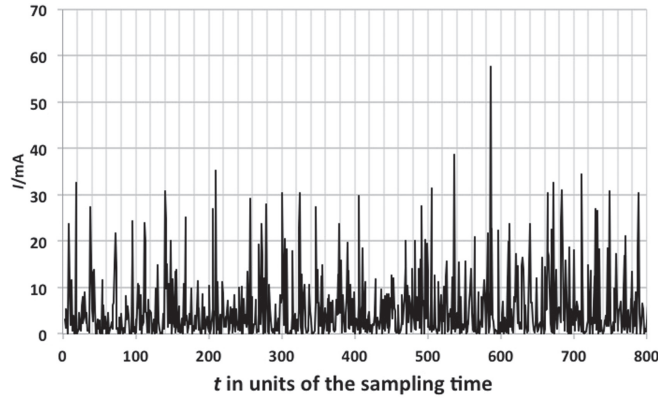


**Figure 10.** A Rayleigh distribution  $P(a)da$  derived from the circularly complex distributed variable  $A$ ;  $\sigma = 2.2 \approx \sigma(AX) = \sigma(AY)$ .

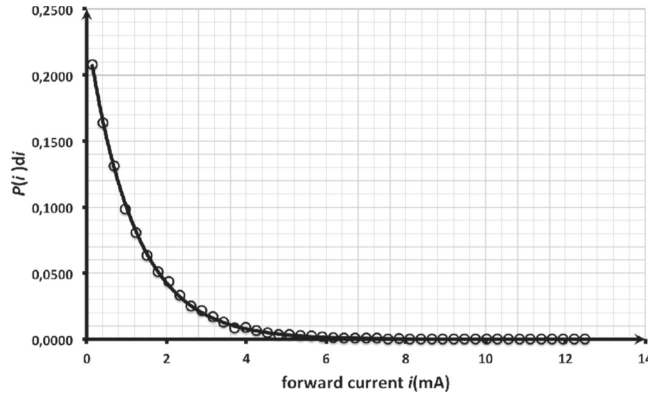
$$P(a = |A|)da = \frac{a}{\sigma^2} \exp\left(-\frac{a^2}{2\sigma^2}\right)da. \quad (18)$$

Figure 10 shows the resulting probability function of the phasor length  $a = |A|$ . The characteristic curve of the LED (L-53SR SUPER BRIGHT RED; GaAl/AS) shows a typical intercept at  $i \approx 0.09$  mA. As a correction we moved the centre slightly away from the zero point. Due to this displacement of the zero point the variance of the Rayleigh distribution measured here ( $\sigma^2 = 4.84$ ) lies a bit above the expected value ( $\sigma^2 = 4.41$ ).

To take into account the squared dependence of the intensity from the field strength we use  $|A|^2$  to modulate the intensity. Thus the electronic set up was designed to produce a forward current proportional to the square of the phasor length. With a phenomenological proportionality constant  $\alpha^*$  we write:  $i = \alpha^*|A|^2$ . Now from  $P(a)da$  we calculate the random distribution of the current  $P(i)di$



**Figure 11.** Times series of the forward current  $i(t)$ ; sampling time  $\tau_D = 20 \mu\text{s}$ ,  $t$  is given in units of  $\tau_D$ .



**Figure 12.** Exponential distribution of the forward current shown in figure 11; statistical parameters are  $\sigma(i) = \langle i \rangle = 1.28 \text{ mA}$ .

$$P(i)di = P\left(a = \sqrt{\frac{i}{\alpha^*}}\right) \frac{da}{di} = \frac{1}{2\alpha^*\sigma^2} \exp\left(-\frac{i}{2\alpha^*\sigma^2}\right) di = \frac{1}{\langle i \rangle} \exp\left(-\frac{i}{\langle i \rangle}\right) di. \quad (19)$$

As expected we find the exponential distribution given in equation (19). The fit yields  $\sigma(i) = \langle i \rangle = 1.28 \text{ mA}$ ; from theory we should find  $\langle i \rangle = 2 \cdot \alpha^* |A|^2 = 2 \cdot 33.5 \text{ mA}/255 \cdot \sigma^2 = 1.27 \text{ mA}$ . Figure 12 demonstrates the perfect fit between the experimental results and the statistical theory. Within the low intensity regime we used, the LED intensity  $I_{\text{ca}}$  follows linearly:  $I_{\text{ca}} \propto i$  (see first LED experiment). Nothing extraordinary will happen here.

The last step describes the production of photo counts, i. e. the number of photoelectrons  $m$  from the PM during time  $\tau_D$ . Figure 13 shows the perfect geometrical distribution  $P(m, \tau_D)$  as expected from the exponential in figure 12. Details of the PF  $P(m, \tau_D)$  could be directly derived from the single experimental parameter  $\langle m \rangle$  (see appendix B)

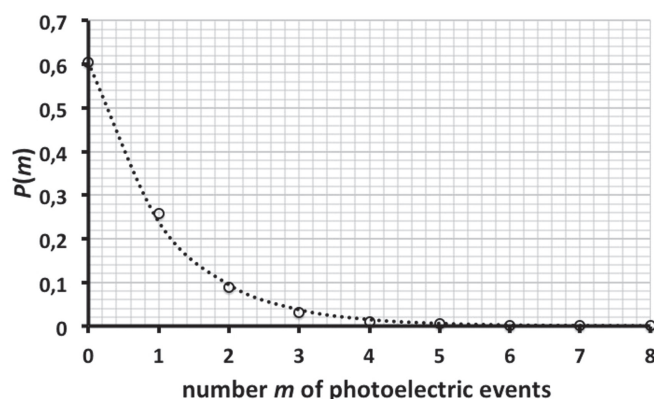


**Figure 13.** Geometrically distributed photo counts in the case of chaotic intensity fluctuations; measurement: open circles, theoretically expected values: dotted line.

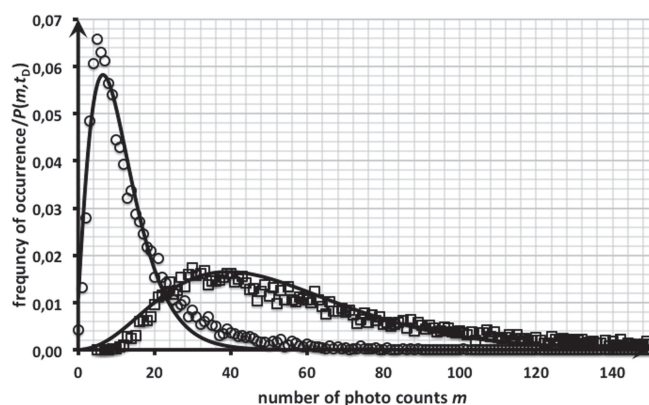


**Figure 14.** Two experimental results using a long sampling period:  $\tau_D = 1$  ms (circles) and  $\tau_D = 4$  ms (squares); the coherence time has been estimated to  $\tau_C = 1$  ms.

$$P(m) = \frac{\langle m \rangle^m}{(1 + \langle m \rangle)^{1+m}}; \langle m \rangle = \xi \cdot \tau_D \cdot \langle I_{ca}(t) \rangle. \quad (20)$$

Finally we ask for the influence of the sampling period  $\tau_D$ . Figures 13 and 14 give some experimental results and theoretical fits.

$\tau_D = 20 \mu\text{s}$	$q = 1$ ; one coherence cell per sampling period	Figure 13
$\tau_D = 1.0 \text{ ms}$	$q = 2.7$	Figure 14
$\tau_D = 4.0 \text{ ms}$	$q = 4.1$	Figure 14

As could be seen, we could not achieve a perfect fit. A main reason for this lack of fitting quality is because the theoretical approach is a bit crude. The derivation of equation (12) starts with a number of coherence cells  $q$  restricted to integer values. Finally we are fitting the measurements with real  $q$ -numbers via the Euler gamma function  $\Gamma(q)$  instead of factorial  $q!$  (see [10, 11]). A further assumption uses  $n \gg q$  (see appendix B); the integration in

equation (13) to derive  $P(m, \tau_D)$  however includes  $I = 0$ . Though the approximations are not totally consistent, we find the theoretical ideas matching the experimental results broadly satisfactory. To improve the consistency between the theoretical model and experiments we have to find a better way to characterise the light field, and a less crude approximation of the probability function of the light field especially for small light intensities.

#### 4. Conclusion

We demonstrated a series of undergraduate experiments well suited to enlightening methods of statistical optics.

- Experiment 1: a change of the perspective in a standard x-ray experiment gives the first steps to ‘counting light’ in statistical optics.
- Experiment 2: the rotating diffuser shows the influence of coherence characteristics ‘in principle’ and demonstrates the role of spatial coherence.
- Experiment 3: finally, less complicated LED experiments open the door to statistical models of the physics of photoelectron devices.

All these experiments rely on the theory of random variables in optical sciences.

The experiments described here are designed to fit the skills of second-year students (BSc. physics). Therefore we tried to sidestep the use of the term photon. Sometimes, especially for x-ray-experiments, this way seems to be a bit unusual. This practice is however well justified, as all learners tend to melt together their beliefs and their sciolism with clear distinct knowledge from the lessons. Especially in the later quantum physics course photon misconceptions will lead to lots of discussions beside 2-level-atoms and the theory of radiation. In order to avoid confusion we try to argue without photons on this level.

We often experience in the classroom that quantum optics turns out to be an very elusive issue, it aggravates the educational situation of the students and makes it much more difficult to draw their mind into closer touch with the concepts and curiosities of quantum physics when they do not have a stable background in statistical methods in physics.

The educational approach shown here delivers a clear background in statistical optics. We restricted ourselves to pure intensity measurements. The experiments should consequently be continued to coincidence measurements in classical physics and will directly lead to single-photon-experiments in quantum optics. The main disadvantage of this approach is obvious: one misses the term photon. There are some kernel points relying on at least some naive idea of photons:

- they carry energy given by  $h \cdot f$ ;
- they are indivisible;
- they populate minimal volumes, co called coherence cells, in a grainy phase space (see appendix C).

For example there is an interesting field around the  $q$ -value-experiments. These experiments are well suited to give detailed insight into spectroscopic features (characteristic of the spectral line, coherence time) from the statistical point of view. We will report on this subject later.

## Acknowledgments

The authors wish to thank the student Daniel Hildebrandt for preliminary work and ideas. They are also grateful for the valuable and detailed feedback from the two reviewers.

## Appendix. Simplified derivation of central formulas

### Appendix A. Fluctuations in thermal equilibrium

To derive equation (1) we start with the canonical ensemble (Gibbs ensemble) at temperature  $T$  (thermal equilibrium). In this case the classical probability to find the system in the state  $j$  with a mean energy  $W_j$  is given by the Boltzmann distribution

$$P_j = \frac{1}{Z} \exp\left(-\frac{W_j}{k_B T}\right); \quad Z = \sum_n \exp\left(-\frac{W_n}{k_B T}\right). \quad (\text{A1})$$

Elementary statistics tells us how equation (A1) can be used to calculate mean values. Thus we get for the mean energy and higher statistical momenta

$$\langle W \rangle = \sum_n W_n P_n = \frac{1}{Z} \sum_n W_n \exp(-\beta W_n) = -\frac{\partial}{\partial \beta} \ln(Z). \quad (\text{A2})$$

and, using the abbreviation  $\beta = 1/(k_B T)$

$$\frac{\partial}{\partial \beta} \langle W \rangle = \frac{1}{Z^2} \left(\frac{\partial Z}{\partial \beta}\right)^2 - \frac{1}{Z} \frac{\partial^2 Z}{\partial \beta^2} = \langle W \rangle^2 - \frac{1}{Z} \sum_n W_n^2 \exp(-\beta W_n) = \langle W \rangle^2 - \langle W^2 \rangle. \quad (\text{A3})$$

Inserting for  $\beta$  we finally get equation (1)

$$\begin{aligned} \frac{\partial}{\partial \beta} \langle W \rangle &= \frac{1}{Z^2} \left(\frac{\partial Z}{\partial \beta}\right)^2 - \frac{1}{Z} \frac{\partial^2 Z}{\partial \beta^2} = \langle W \rangle^2 - \frac{1}{Z} \sum_n W_n^2 \exp(-\beta W_n) = \langle W \rangle^2 - \langle W^2 \rangle. \\ \langle W^2 \rangle - \langle W \rangle^2 &= -\frac{\partial}{\partial \beta} \langle W \rangle = -\frac{\partial}{\partial T} \frac{\partial T}{\partial \beta} \langle W \rangle = k_B T^2 \frac{\partial}{\partial T} \langle W \rangle. \end{aligned} \quad (\text{A4})$$

Now, with Plank's law for the mean energy  $\langle W \rangle$ , we derive equation (2) for the fluctuations of the thermal radiation field

$$\begin{aligned} \langle W \rangle &= V \cdot \frac{\hbar \omega^3}{\pi^2 c^3} \frac{1}{\exp(\hbar \omega / k_B T) - 1} \Rightarrow \\ \langle W^2 \rangle - \langle W \rangle^2 &= k_B T^2 \frac{\partial}{\partial T} \langle W \rangle = k_B T^2 V \cdot \frac{\hbar \omega^3}{\pi^2 c^3} \frac{\hbar \omega / k_B T^2 \exp(\hbar \omega / k_B T)}{(\exp(\hbar \omega / k_B T) - 1)^2} \\ &= \langle W \rangle^2 \cdot \frac{\pi^2 c^3}{V \hbar \omega^3} \cdot \hbar \omega \cdot [\exp(\hbar \omega / k_B T) - 1 + 1] \\ &= \left( \hbar \omega + \frac{\pi^2 c^3}{V \omega^2} \langle W \rangle \right) \langle W \rangle. \end{aligned} \quad (\text{A5})$$

## Appendix B. The detector signal $P(m, \tau_D)$

Within the semi-classical theory we assume that the probability  $p(t)dt$  produces a photoelectron is proportional to the cycle-averaged intensity,  $p(t)dt = \xi I_{ca} dt$  (see the table of constants in section 2). A laser with constant intensity acts like a radioactive source with constant activity. The detection process will recognize a Poissonian-like distributed probability  $P(m; t; \tau_D)$  to get exact  $m$  photoelectrons during time  $\tau_D$  [7, p 119 ff]

$$P(m, t, \tau_D) = \frac{(\xi \tau_D I_{ca}(t, \tau_D))^m}{m!} \exp(-\xi \tau_D I_{ca}(t, \tau_D)). \quad (\text{B1})$$

The sampling process of the detection system is represented by the integration

$$I_{ca}(t, \tau_D) = \frac{1}{\tau_D} \int_t^{t+\tau_D} dt' I_{ca}(t').$$

For the case of fluctuating light we have to average the distribution (B1) over all points of time  $t$

$$P(m, \tau_D) = \left\langle \frac{(\xi \tau_D I_{ca}(t, \tau_D))^m}{m!} \exp(-\xi \tau_D I_{ca}(t, \tau_D)) \right\rangle_t. \quad (\text{B2})$$

From equation (B2) it follows immediately the mean number of counts due to the normalization condition

$$\begin{aligned} \langle m \rangle &= \sum_{M=0}^{\infty} M \cdot P(M, \tau_D) = \left\langle \sum_{M=0}^{\infty} M \frac{(\xi \tau_D I_{ca}(t, \tau_D))^M}{M!} \exp(-\xi \tau_D I_{ca}(t, \tau_D)) \right\rangle_t \\ &= \left\langle (\xi \tau_D I_{ca}(t, \tau_D)) \sum_{M=1}^{\infty} \frac{(\xi \tau_D I_{ca}(t, \tau_D))^{M-1}}{(M-1)!} \exp(-\xi \tau_D I_{ca}(t, \tau_D)) \right\rangle_t \\ &= \xi \tau_D \langle I_{ca}(t, \tau_D) \rangle_t. \end{aligned} \quad (\text{B3})$$

Equation (B2) is Mandel's famous formula [7]. In some cases (look for 'stationary ergodic light' in the literature) the average value (B2) is given by the expectation value of equation (B1) weighted by the probability distribution of the incoming light intensity. With  $P(I_{ca})dI_{ca}$  for the probability to find an cycle averaged intensity between  $I$  and  $I + dI$ ,  $P(m, \tau_D)$  is derived from equation (B2)

$$P(m, \tau_D) = \int_0^{\infty} dI_{ca} P(I_{ca}) \frac{(\xi \tau_D I_{ca}(t, \tau_D))^m}{m!} \exp(-\xi \tau_D I_{ca}(t, \tau_D)). \quad (\text{B4})$$

For an ideal laser we have a constant intensity; the mean number of counts is given by  $\langle m \rangle = \xi \tau_D \langle I_{ca}(t, \tau_D) \rangle = \xi \tau_D \langle I_{laser}(t, \tau_D) \rangle = \xi \tau_D I_{laser}$  and the intensity distribution is given by the delta function  $P(I_{ca}, t, \tau_D)dI_{ca} = \delta(I_{ca} - I_{laser})dI_{ca}$ . We get from equation (B4) the well known Poissonian

$$\begin{aligned} P(m, \tau_D) &= \int_0^{\infty} dI_{ca} \delta(I_{ca}(t, \tau_D) - I_{laser}) \frac{(\xi \tau_D I_{ca}(t, \tau_D))^m}{m!} \exp(-\xi \tau_D I_{ca}(t, \tau_D)) \\ &= \frac{(\xi \tau_D I_{laser})^m}{m!} \exp(-\xi \tau_D I_{laser}) = \frac{\langle m \rangle^m}{m!} \exp(-\langle m \rangle). \end{aligned} \quad (\text{B5})$$

For the case of thermal/chaotic light we may find for the intensity distribution the exponential (see appendix D)

$$P(I_{ca}(t, \tau_D))dI_{ca} = \frac{1}{\langle I_{ca}(t, \tau_D) \rangle} \exp\left(-\frac{I_{ca}(t, \tau_D)}{\langle I_{ca}(t, \tau_D) \rangle}\right)dI_{ca}. \quad (\text{B6})$$

With  $\langle m \rangle = \langle \xi \tau_D I_{ca}(t, \tau_D) \rangle$  and  $\int_0^\infty dx x^n \exp(-ax) = \frac{n!}{a^{n+1}}$  we can calculate the integral in equation (B4) and finally obtain a geometrical distribution for the probability of measuring  $m$  photoelectrons from the PM during time  $\tau_D$

$$\begin{aligned} P(m, \tau_D) &= \int_0^\infty dI_{ca} P(I_{ca}(t, \tau_D)) \frac{(\xi \tau_D I_{ca}(t, \tau_D))^m}{m!} \exp(-\xi \tau_D I_{ca}(t, \tau_D)) \\ &= \int_0^\infty dI_{ca} \frac{1}{\langle I_{ca}(t, \tau_D) \rangle} \exp\left(-\frac{I_{ca}(t, \tau_D)}{\langle I_{ca}(t, \tau_D) \rangle}\right) \frac{(\xi \tau_D I_{ca}(t, \tau_D))^m}{m!} \\ &\quad \times \exp(-\xi \tau_D I_{ca}(t, \tau_D)) \\ &= \frac{(\xi \tau_D)^m}{\langle I_{ca}(t, \tau_D) \rangle} \frac{1}{m!} \int_0^\infty dI_{ca} (I_{ca}(t, \tau_D))^m \\ &\quad \times \exp\left(-I_{ca}(t, \tau_D) \left(\xi \tau_D + \frac{1}{\langle I_{ca}(t, \tau_D) \rangle}\right)\right) \\ &= \frac{(\xi \tau_D)^m}{\langle I_{ca}(t, \tau_D) \rangle} \frac{1}{m!} \int_0^\infty dI_{ca} (I_{ca}(t, \tau_D))^m \\ &\quad \times \exp\left(-I_{ca}(t, \tau_D) \left(\frac{\xi \tau_D \cdot \langle I_{ca}(t, \tau_D) \rangle + 1}{\langle I_{ca}(t, \tau_D) \rangle}\right)\right) \\ &= \frac{(\xi \tau_D)^m}{\langle I_{ca}(t, \tau_D) \rangle} \frac{1}{m!} \cdot \frac{m! \langle I_{ca}(t, \tau_D) \rangle^{m+1}}{(1 + \xi \tau_D \langle I_{ca}(t, \tau_D) \rangle)^{m+1}} = \frac{\langle m \rangle^m}{(1 + \langle m \rangle)^{m+1}}. \end{aligned} \quad (\text{B7})$$

### Appendix C. Counting statistics: the concept of coherence cells

A typical optical-counting-experiment relies on the counting of the number of voltage signals ('photoelectrons') during some detection time  $\tau_D$ . The number of detected photoelectrons  $m$  is usually thought to be correlated to the cycle-averaged intensity by ( $\omega = 2 \cdot \pi \cdot f$  represents the *mid frequency* of the radiation field, the *coherence volume* is given by  $V_C = A_C \cdot c \cdot \tau_C$  estimates the spatial expansion of so called *coherence cells*)

$$m(t, \tau_D) = \eta \cdot \frac{A_C}{\hbar \omega} \tau_D I_{ca}(t, \tau_D) = \xi \tau_D I_{ca}(t, \tau_D). \quad (\text{C1})$$

For the special case of a chaotic (or thermal) light source we expect geometrical distributed numbers of photoelectrons [8]

$$P(m, \tau_D) = \frac{\langle m \rangle^m}{(1 + \langle m \rangle)^{1+m}}. \quad (\text{C2})$$

Equations (B6) and (B7) are valid only for a detection time  $\tau_D < \tau_C$ . However, due to a rather small coherence time  $\tau_C \approx h/(k_B T)$  we usually have  $\tau_D \gg \tau_C$ , the intensity fluctuations wash out and we will measure virtually constant intensity on the detector. Thus it is experimentally challenging to realize  $\tau_D < \tau_C$  in the thermal region at least in undergraduate experiments. Therefore it is interesting to find ways to realize  $\tau_D < \tau_C$  as shown in the experiment with so called *pseudo thermal light* ([6] and [10]).

Here we demonstrate a path to understand how elementary statistics can be used to construct a light field with pseudo thermal characteristics.

Step 1: the number of photons.

The number of energy packets  $\hbar\omega$  (for simplicity we call them photons) contained in the coherence cell number  $i$  of the light beam of intensity  $I_{ca}(t)$  may be denoted by  $n_i(t)$ . Now we assume that the mean value of photons per coherence cell,  $\langle n_i(t) \rangle$ , is the same for each coherence cell

$$I_{ca}(t) = \frac{c}{V_C} \cdot \langle n_i(t) \rangle \cdot \hbar\omega = \frac{\langle n_i(t) \rangle \cdot \hbar\omega}{A_C \cdot \tau_C}. \quad (C3)$$

Step 2: the concept of coherence cells.

Let us go further with the assumption that the photons of the light beam are distributed uniformly over independent coherence cells.  $q$  of them, with a total number  $n(t, \tau_D)$  of photons are sampled during the sampling period  $\tau_D$  by the detector. Each coherence cell carries a mean value of photons given by  $\langle n_i(t) \rangle$

$$\left. \begin{aligned} n(t, \tau_D) \cdot \hbar\omega &= q \cdot \langle n_i(t) \rangle \cdot \hbar\omega = q I_{ca}(t) \cdot A_C \cdot \tau_C \\ n(t, \tau_D) &= \frac{I_{ca}(t)}{\hbar\omega} A_C \cdot \tau_C \end{aligned} \right\} \Rightarrow q = \frac{\tau_D}{\tau_C}. \quad (C4)$$

Step 3: the probability distribution of the  $n_i(t)$ .

For the case of thermal light we have to start with geometrically distributed photon numbers for each cell

$$P(n_i) = \frac{\langle n_i \rangle^{n_i}}{(1 + \langle n_i \rangle)^{1+n_i}} = \frac{1}{(1 + \langle n_i \rangle)} \cdot \frac{1}{(1 + 1/\langle n_i \rangle)^{n_i}}. \quad (C5)$$

Step 4: the probability to find  $n$  photons during time  $\tau_D$ .

Now different distributions from different coherence cells are statistically independent. The total probability for one realisation of a specific  $(n, q)$ -constellation is therefore given by the product

$$\begin{aligned} \tilde{P}(n, q) &= \prod_1^q P(n_i) = \prod_1^q \frac{1}{(1 + \langle n_i \rangle)} \cdot \frac{1}{(1 + 1/\langle n_i \rangle)^{n_i}} = \frac{1}{(1 + \langle n_i \rangle)^q} \cdot \frac{1}{(1 + 1/\langle n_i \rangle)^n} \\ &= \frac{1}{\left(1 + \frac{\langle n \rangle}{q}\right)^q} \cdot \frac{1}{\left(1 + \frac{q}{\langle n \rangle}\right)^n}. \end{aligned} \quad (C6)$$

Finally we have to multiply the probability with the number of different realizations of the  $(n, q)$ -constellation and finally get the so called *negative-binomial distribution*

$$\begin{aligned}
P(n, q) &= \frac{(n+q-1)!}{n!(q-1)!} \cdot \frac{1}{\left(1 + \frac{\langle n \rangle}{q}\right)^q} \cdot \frac{1}{\left(1 + \frac{q}{\langle n \rangle}\right)^n} \\
&= \frac{\Gamma(n+q)}{\Gamma(n+1) \cdot \Gamma(q)} \cdot \frac{1}{\left(1 + \frac{\langle n \rangle}{q}\right)^q} \cdot \frac{1}{\left(1 + \frac{q}{\langle n \rangle}\right)^n}. \quad (\text{C7})
\end{aligned}$$

Some remarks.

- For  $q = 1$  one finds the geometrical distribution formula equation (B1).
- The derivation of equation (C7) uses as well that  $q$  should be given by a positive integer as the idea  $q = \tau_D/\tau_C$ . It seems a to be a bit curious. However equation (C7) can be derived from a more generalized point of view without the restriction of  $q$  to be positive integer (see [6, p 176] for details).

Now for small numbers of coherence cells compared to the mean number of photons we can get rid of the number of photons in the exponent

$$\begin{aligned}
P(n, q) &= \frac{\Gamma(n+q)}{\Gamma(n+1) \cdot \Gamma(q)} \cdot \frac{1}{\left(1 + \frac{\langle n \rangle}{q}\right)^q} \cdot \frac{1}{\left(1 + \frac{q}{\langle n \rangle}\right)^n} \\
&\approx \frac{\Gamma(n+q)}{\Gamma(n+1) \cdot \Gamma(q)} \left(\frac{q}{\langle n \rangle}\right)^q \cdot \exp\left(-\frac{q}{\langle n \rangle} \cdot n\right) \\
&\approx \frac{1}{\Gamma(q)} \frac{n^{q-1}}{\langle n \rangle^q} \left(\frac{q}{\langle n \rangle}\right)^q \cdot \exp\left(-\frac{q}{\langle n \rangle} \cdot n\right). \quad (\text{C8})
\end{aligned}$$

Inserting  $n(t, \tau_D) = \frac{I_{ca}(t, \tau_D)}{\hbar\omega} A_C \tau_D = \frac{I_{ca}(t, \tau_D)}{\eta}$  we derive the intensity distribution

$$\begin{aligned}
P(I_{ca}(t, \tau_D)) dI_{ca} &= P(n = I_{ca}(t, \tau_D)/\eta) \frac{dn}{dI_{ca}} dI_{ca} \\
&= \frac{q^q}{\Gamma(q)} \frac{I_{ca}(t, \tau_D)^{q-1}}{\langle I_{ca}(t, \tau_D) \rangle^q} \exp\left(-\frac{q I_{ca}(t, \tau_D)}{\langle I_{ca}(t, \tau_D) \rangle}\right) dI_{ca}. \quad (\text{C9})
\end{aligned}$$

Again for  $q = 1$  one obtains the one-cell-case given in equation (B6).

Equation (C9) gives the distribution of the radiation intensity. However, we measure the distribution of counts from a binary counter. Thus we have to insert into Mandel's formula, equation (8), and obtain the final distribution  $P(m, \tau_D)$

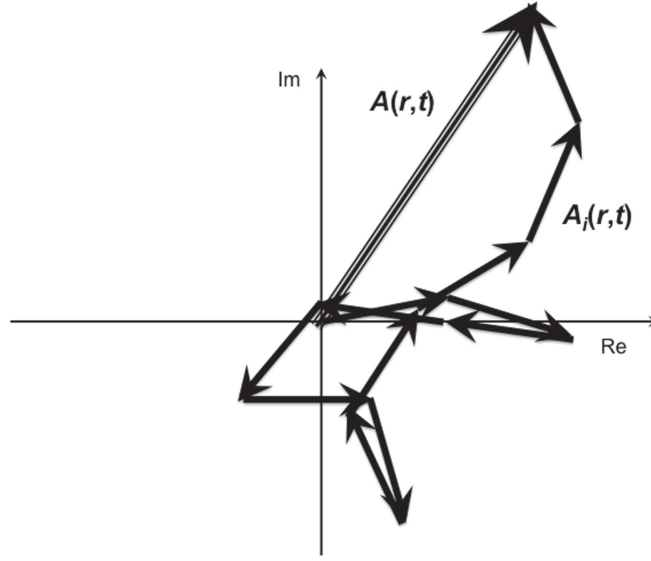


**Figure D1.** Complex amplitudes with random phases add to the resultant field.

$$\begin{aligned}
 P(m, \tau_D) &= \int_0^\infty dI_{ca} P(I_{ca}) \frac{(\xi \tau_D I_{ca}(t, \tau_D))^m}{m!} \exp(-\xi \tau_D I_{ca}(t, \tau_D)) \\
 &= \int_0^\infty dI_{ca} \frac{q^q}{\Gamma(q)} \frac{I_{ca}(t, \tau_D)^{q-1}}{\langle I_{ca}(t, \tau_D) \rangle^q} \exp\left(-\frac{q I_{ca}(t, \tau_D)}{\langle I_{ca}(t, \tau_D) \rangle}\right) \frac{(\xi \tau_D I_{ca}(t, \tau_D))^m}{m!} \\
 &\quad \times \exp(-\xi \tau_D I_{ca}(t, \tau_D)) \\
 &= \frac{q^q}{\Gamma(q)} \frac{(\xi \tau_D I_{ca})^m}{\langle I_{ca}(t, \tau_D) \rangle^q m!} \int_0^\infty dI_{ca} \exp\left(-\frac{q I_{ca}(t, \tau_D)}{\langle I_{ca}(t, \tau_D) \rangle}\right) \frac{(I_{ca}(t, \tau_D))^{m+q-1}}{m!} \\
 &\quad \times \exp\left(-I_{ca}(t, \tau_D) \left(\xi \tau_D + \frac{q}{\langle I_{ca}(t, \tau_D) \rangle}\right)\right) \\
 &= \frac{\Gamma(m+q)}{\Gamma(m+1)\Gamma(q)} \left(1 + \frac{q}{\langle m \rangle}\right)^{-m} \left(1 + \frac{\langle m \rangle}{q}\right)^{-q} \\
 &= \binom{m+q-1}{m} \left(1 + \frac{q}{\langle m \rangle}\right)^{-m} \left(1 + \frac{\langle m \rangle}{q}\right)^{-q}.
 \end{aligned} \tag{C10}$$

Equation (C10) equals the negative binomial distribution derived in [6, p 178]. Fitting the values of  $q$  even for the continuous case we may estimate the influence of the additional coherence-cell-contributions. As stated above equation (C10) may become a little problematic in the medium range of  $\tau_D \approx \tau_C$  and for low values of  $\langle m \rangle$  because of a breakdown of the approximations.

#### Appendix D. The random-phasor-model

As shown in figure D1 the resultant field amplitude  $A(r, t)$  is calculated from a large number of contributions with a random phase and length.

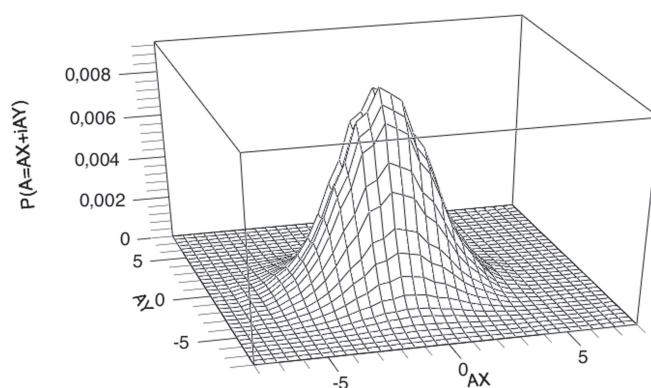


**Figure D2.** The random phasor model:  $A$  is constructed as a circular complex gaussian variable  $A = AX + iAY$ ; with  $\langle AX \rangle = \langle AY \rangle = 0$  and  $\sigma^2(AX) = \sigma^2(AY) = 4.3$ .

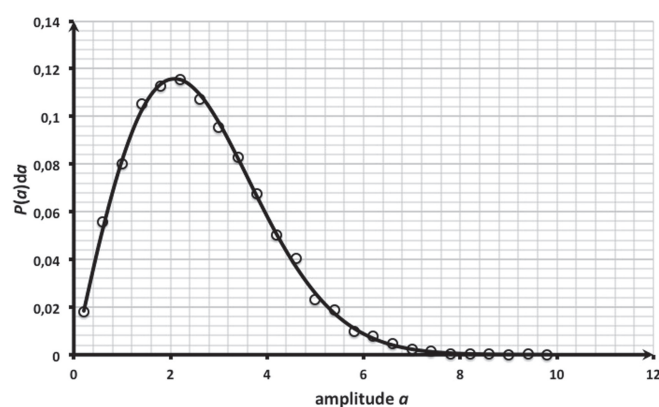


**Figure D3.** The Raleigh distribution for  $a = |A|$  as given by equation (C1) for  $\sigma^2 = \sigma^2(AX) = \sigma^2(AY) = 4.3$ ; the dots are derived from the distribution figure D2.

$$A(r, t) = \sum_i (\text{Re}(A_i(r, t)) + i\text{Im}(A_i(r, t))). \quad (\text{D1})$$

The complex phasor  $A$  is constructed as a circular complex Gaussian random variable (see figure D2)

$$A = AX + iAY; \langle AX \rangle = \langle AY \rangle = 0; \text{var}(AX) = \text{var}(AY) = \sigma^2$$

$$P(A)dA = \frac{1}{2\pi\sigma^2} \exp\left(-\frac{AX^2 + AY^2}{2\sigma^2}\right). \quad (\text{D2})$$

It then follows from elementary statistics [1] that  $a = |A|$  is Rayleigh distributed (figure D3)

$$P(a = |A|)da = \frac{a}{\sigma^2} \exp\left(-\frac{a^2}{2\sigma^2}\right)da \quad (\text{D3})$$

where  $\sigma^2$  equals the variance of the Im- and Re-part of the amplitude.

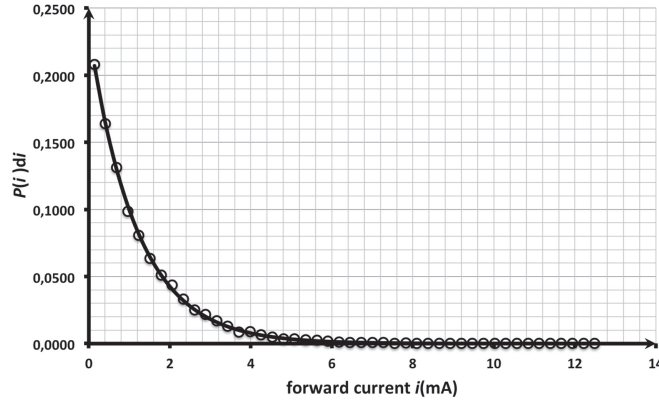


**Figure D4.** Exponential distribution of the modulating current  $i$ ;  $\langle i \rangle = \sigma(i) = 1.18$  mA.

This amplitude can be used to modulate the forward current of the LED. For this purpose we divided the range  $0 < |A|^2 < |A|_{\max}^2$  digitally into 256 steps and adjusted a simple DA-transformer to give  $I = 33,5$  mA for  $|A|^2 = 255$ , thus we have  $I = \alpha^* \cdot |A|^2$ , with a scaling factor  $\alpha^* = 33,5$  mA/255.

Using  $I = \alpha^* \cdot |A|^2$  we can easily calculate the distribution of the LED-forward current from equation (D3) (see figure D4):

$$\begin{aligned} P(i)di &= P\left(a = \sqrt{\frac{i}{\alpha^*}}\right) \frac{da}{di} = \frac{1}{2\alpha^*\sigma^2} \exp\left(-\frac{i}{2\alpha^*\sigma^2}\right) di \\ &= \frac{1}{\langle i \rangle} \exp\left(-\frac{i}{\langle i \rangle}\right) di. \end{aligned} \quad (\text{D4})$$

The standard deviation  $\sigma(i) = \langle i \rangle$  of the forward current distribution may be determined from the Rayleigh parameter  $\sigma^2(i) = \langle i \rangle = \alpha^* \cdot 2\sigma^2 = 1,18$  mA.

With  $I = \alpha \cdot i$  for the LED-intensity we finally get the probability distribution of the LED-intensity

$$P(I_{ca})dI_{ca} = P(i = I_{ca}/\alpha_i) \frac{di}{dI_{ca}} dI_{ca} = \frac{1}{\langle I_{ca} \rangle} \exp\left(-\frac{I_{ca}}{\langle I_{ca} \rangle}\right) dI_{ca}. \quad (\text{D5})$$

This is identical to the distribution we get from the geometrical distribution for the photon number  $n$  for large  $n$

$$\begin{aligned} P(n) &= \frac{\langle n \rangle^n}{(1 + \langle n \rangle)^{1+n}} = \frac{1}{(1 + \langle n \rangle)} \frac{\langle n \rangle^n}{(1 + \langle n \rangle)^n} = \frac{1}{(1 + \langle n \rangle)} (1 + 1/\langle n \rangle)^{-n} \\ &\rightarrow \frac{1}{\langle n \rangle} \exp(-n/\langle n \rangle) \Rightarrow \\ P(I_{ca}) &= \frac{dI_{ca}}{\langle I_{ca} \rangle} \exp(-I_{ca}/\langle I_{ca} \rangle). \end{aligned} \quad (\text{D6})$$

## References

- [1] Forrester A T, Gudmudsen R A and Johnson P O 1955 Photoelectric mixing of incoherent light *Phys. Rev.* **99** 1691
- [2] Hanbury Brown R and Twiss R R 1956 Correlation between photons in two coherent beams of light *Nature* **177** 27
- [3] Hanbury Brown R and Twiss R R 1956 A test of a new type of stellar interferometer on sirius *Nature* **178** 1046
- [4] Goodman J W 2000 *Statistical Optics* (New York: John Wiley & Sons Inc.)
- [5] Einstein A 1909 On the present status of the radiation problem *Phys. Z* **10** 185–93
- [6] Saleh B 1978 *Photoelectron Statistic* (Berlin: Springer)
- [7] Mandel L 1958 Fluctuations of photon beams and their correlation *Proc. Phys. Soc.* **72** 1037
- [8] Loudon R 2006 *The Quantum Theory of Light* 3rd edn (Oxford: Oxford Science Publications)
- [9] Martienssen W and Spiller E 1964 Coherence and fluctuations in light beams *Am. J. Phys.* **32** 919
- [10] Wolf R P and Crooker P P P P 1982 Fluctuations in light beams: a simple student experiment *Am. J. Phys.* **50** 406
- [11] Troup G J 1965 Coherent intensity distributions from boson statistics *Proc. Phys. Soc.* **86** 39
- [12] Saleh B and Teich M C 1991 *Fundamentals of Photonics* (New York: John Wiley & Sons Inc.)
- [13] Leutner S, Scholz R and Friege G 2010 Einsatz eines Mach–Zehnder-interferometers mit abgeschwächter Lichtquelle für einen experimentellen Einstieg in die Quantenmechanik *Phy. Did. B* (<http://www.phydid.de/index.php/phydid-b/article/view/175/214>)
- [14] Goodman J W 1976 Some fundamental properties of speckle *J. Opt. Soc. Am.* **66** 1145
- [15] Born M 1972 *Optik* (Berlin: Springer) ch 2